

# TOPOLOGICAL DEPENDENCE OF UNIVERSAL CORRELATIONS IN MULTI-PARAMETER HAMILTONIANS

David MITCHELL and Dimitri KUSNEZOV<sup>1</sup>

*Center for Theoretical Physics, Sloan Physics Laboratory,  
Yale University, New Haven, CT 06520-8120 USA*

*April 1996*

## ABSTRACT

Universality of correlation functions obtained in parametric random matrix theory is explored in a multi-parameter formalism, through the introduction of a diffusion matrix  $D_{ij}(\mathbf{R})$ , and compared to results from a multi-parameter chaotic model. We show that certain universal correlation functions in 1-d are no longer well defined by the metric distance between the points in parameter space, due to a global topological dependence on the path taken. By computing the density of diabolical points, which is found to increase quadratically with the dimension of the space, we find a universal measure of the density of diabolical points in chaotic systems.

**PACS numbers:** 05.40+j, 05.45+b, 24.60.-k

---

<sup>1</sup>E-mail: dimitri@nst4.physics.yale.edu

# 1. Introduction

The relation between classically chaotic systems and the fluctuation properties of the corresponding quantum systems has been a focus of intense investigation in recent years[1]. We have learned that the quantum counterpart of classically chaotic systems have many properties which can be described by random matrix theory (RMT). As a consequence, one now typically invokes random matrix ensemble averaging to simplify the computation of properties of complex systems. But while the understanding of properties of RMT is now quite well established, until recently very little was known about random matrix or chaotic Hamiltonians which depend on an external parameter  $x$ . The parameter dependence can be the strength of an external field, or even the motion of slow variables in a complex system treated in the Born-Oppenheimer approximation[2]. The types of questions one is interested in are how the properties of such systems are correlated in that parameter. In the past few years it has become apparent that a more general class of random matrix results exist for parametric Hamiltonians. In a series of papers, Szafer-Simons and Altshuler [3] computed the density-density and level velocity correlators in a parametric random matrix model, and demonstrated that it described the behavior of very different chaotic and disordered systems. By introducing a specific scaling of the parameter  $x$ , correlation functions were found to fall upon universal curves, independent of the underlying properties of the studied systems. Since then, there has been extensive studies on universality in other systems, and the class of observables has been extended to include wavefunctions and distributions of matrix elements[4]. Several further studies were based on Ref. [4], including a check that the predictions for wavefunctions hold in chaotic systems[5], a general theory for scaling[6], and the introduction and verification of a wide class of universal correlation functions and distributions[7]. However, all this work has been relegated to one parameter models. The purpose of this paper is to extend the previous results to two or more parameters, and to examine the global topological effects on universal functions due to the multi-dimensional parameter space. We point out that the universality of parametric correlations which emerges on short distance scales can be different from 1-parameter model predictions.

## 2. Geometric Phase for GOE Matrices

We consider multiparameter Hamiltonians which exhibit chaos in some region of parameter space, such that the fluctuation properties of the quantum Hamiltonian in that regime are described by random matrix theory. We will limit the discussion to the gaussian orthogonal ensemble (GOE), or systems with time-reversal symmetry. As a result, the Hamiltonian is a real symmetric matrix, with a non-degenerate eigenvalue spectrum. Consider now the general adiabatic variation of the Hamiltonian  $H(\mathbf{R}(t))$ , where the adiabatic eigenstates are defined as

$$H(\mathbf{R}(t))\psi_n(\mathbf{R}(t)) = E(\mathbf{R}(t))\psi_n(\mathbf{R}(t)). \quad (1)$$

For a wavefunction adiabatically transported along some path  $\mathbf{R}$ , the wavefunction acquires both a dynamical and a geometric phase,  $\gamma$ [8]:

$$\Psi(t) = e^{-(i/\hbar) \int_0^t dt' E_n(\mathbf{R}(t'))} e^{i\gamma_n(t)} \psi_n(\mathbf{R}(t)) \quad (2)$$

We are only concerned here with the geometric component of the acquired phase,  $\gamma_n$ , which contains information about the topology of the parameter space and about the presence of diabolical points. For the parallel transport of the adiabatic states  $\psi_n$  around a closed circuit  $C$  in parameter space, we have

$$\langle \psi_{n,final} | \psi_{n,initial} \rangle = e^{i\gamma_n(C)} \quad (3)$$

For real symmetric matrices, the acquired geometric phase for a closed loop is  $e^{i\gamma(C)} = 1$  if the path does not enclose a degeneracy (diabolical point), and  $e^{i\gamma(C)} = -1$  if the path does enclose a degeneracy[9]. The path can be in any region of parameter space, but if the chaotic properties of the Hamiltonian go away for a particular range of parameter, one might encounter degeneracies and further complications such as non-abelian gauge potentials can develop. We will not consider this here, and hence restrict our discussion to paths in the classically chaotic regions of the model we study, and equivalently, Hamiltonians chosen from the GOE ensemble.

### 3. Two Parameter Models

#### 3.1 RANDOM MATRIX HAMILTONIANS

We first consider a two parameter realization of the GOE ensemble. A convenient Hamiltonian is [10]:

$$H(\mathbf{R}) = H(x, y) = \frac{1}{\sqrt{2}} [H_1 \cos x + H_2 \sin x + H_3 \cos y + H_4 \sin y] , \quad (4)$$

where  $H_\alpha$  are independent,  $N \times N$ , GOE matrices:

$$\begin{aligned} \overline{H_\alpha^{ij}} &= 0 \\ \overline{H_\alpha^{ij} H_\beta^{kl}} &= \frac{a^2}{2} \delta_{\alpha\beta} (\delta_{ik} \delta_{jl} + \delta_{il} \delta_{jk}). \end{aligned} \quad (5)$$

The parameter  $a$  is related to the average level spacing  $\Delta$  via  $a = \Delta\sqrt{N}/\pi$ .  $H(x, y)$  is clearly GOE at every point  $(x, y)$ , and has only two relevant moments:

$$\begin{aligned} \overline{H_{ij}(x, y)} &= 0 \\ \overline{H_{ij}(x, y) H_{kl}(x', y')} &= \frac{a^2}{2} F(x - x', y - y') (\delta_{ik} \delta_{jl} + \delta_{il} \delta_{jk}) , \end{aligned} \quad (6)$$

with

$$F(x, y) = \frac{1}{2} [\cos(x) + \cos(y)] \cong 1 - \frac{1}{4}(x^2 + y^2) + \dots, \quad F(0) = 1. \quad (7)$$

When only one parameter is used Eq. (4), for example keeping  $y$  fixed, we have the equivalent process:

$$\overline{H_{ij}(x)H_{kl}(x')} = \frac{a^2}{2} F(x - x')(\delta_{ik}\delta_{jl} + \delta_{il}\delta_{jk}), \quad (8)$$

where

$$F(x) = \frac{1}{2}(1 + \cos(x)) = \cos^2\left(\frac{x}{2}\right) \cong 1 - \frac{1}{4}x^2 + \dots. \quad (9)$$

### 3.2 A CHAOTIC HAMILTONIAN

We will verify the topological effects we present here in a realistic model. We use the Interacting Boson Model (IBM)[11], which is built from scalar ( $s^\dagger$ ) and quadrupole ( $d_\mu^\dagger, \mu = \pm 2, \pm 1, 0$ ) bosons, which carry angular momentum  $L = 0$  and 2, respectively. This model describes the low energy collective excitations of nuclei with even numbers of protons and neutrons, the bosons representing paired nucleons. In the consistent-Q form[12], the Hamiltonian has only two relevant parameters  $\eta$  and  $\chi$ , and in spherical tensor notation, is given by:

$$H_{ibm}(\eta, \chi) = E_0 + \eta \hat{n}_d + \frac{1 - \eta}{N_b} \hat{\mathbf{Q}}^x \cdot \hat{\mathbf{Q}}^x + c_3 \hat{\mathbf{L}} \cdot \hat{\mathbf{L}}, \quad (10)$$

Here  $\hat{n}_d = d^\dagger \cdot \tilde{d}$  is the  $d$ -boson number operator,  $\hat{L}_\mu = \sqrt{10}[d^\dagger \times \tilde{d}]_\mu^{(1)}$  is the angular momentum,  $N_b$  is the boson number defined as half the number of valence nucleons, and  $\hat{Q}_\mu^x = d_\mu^\dagger s + s^\dagger \tilde{d}_\mu + \chi[d^\dagger \times \tilde{d}]_\mu^{(2)}$  is the quadrupole operator. Because angular momentum is a good quantum number, the parameter  $c_3$  adds only an overall constant to  $H_{ibm}$ , and is unimportant. The typical physical range of the parameters is  $-\sqrt{7}/2 \leq \chi \leq 0$  and  $0 \leq \eta \leq 1$ . The chaotic parameter range of this model has been mapped out in detail[13], and we consider the quantum properties for this classically chaotic regime. The Hamiltonian is diagonalized in the vibrational (or  $U(5)$ ) basis, with  $N_b = 25$ . The universality of one-parameter random matrix theory predictions for wavefunctions and distributions has been established for this model and is extensively discussed in Ref. [7].

### 3.2 TOPOLOGICAL CONSIDERATIONS

The topological properties of the parameter space can be readily taken into account using a symplectic 2-form  $\sigma_{ij}$  and a metric tensor  $g_{ij}$ . The general Riemannian structure of the manifold of quantum states have been defined in Ref. [14]. In the adiabatic basis  $|\psi_n(\mathbf{R})\rangle$  of  $H(\mathbf{R})$ , these are determined by the real and imaginary parts of the quantum geometric tensor[8, 14]:

$$T_{ij} = \langle \nabla_i \psi_n | (1 - |\psi_n\rangle\langle \psi_n|) | \nabla_j \psi_n \rangle = g_{ij} + \frac{i}{2} \sigma_{ij}. \quad (11)$$

The antisymmetric tensor  $\sigma_{ij}$  is related to the element of area of parametric loops we study below, and the metric  $g_{ij}$ , the measure of distance:

$$d\sigma = \sigma_{ij}dR_i \wedge dR_j, \quad ds^2 = g_{ij}dR_idR_j. \quad (12)$$

It is hence possible to incorporate the topological properties of the parameter space into a very general formalism. However, as the random matrix model we consider here, in the universal regime, is rather simple, we forgo a covariant construction in this article.

### 3.4 UNIVERSAL SCALING FOR MULTIPARAMETER THEORIES

Scaling of the parameters is the crucial element in obtaining universality in 1-parameter theories. We need to extend this to multi-parameter models. Consider the short distance diffusion of the adiabatic energies of a Hamiltonian  $H(\mathbf{R})$ . From perturbation theory, following the arguments of Dyson[4, 15, 6] we have to first order:

$$E_n(\mathbf{R}') = E_n(\mathbf{R}) + H_{nn}(\mathbf{R}') - H_{nn}(\mathbf{R}) + \dots \quad (13)$$

It is convenient to rescale the energies by the mean level spacing  $E_n \rightarrow E_n/\Delta$ , so that :

$$\begin{aligned} \overline{(\delta E_n)^2} &= \overline{(E_n(\mathbf{R}') - E_n(\mathbf{R}))^2} \cong \frac{1}{\Delta^2} \overline{(H_{nn}(\mathbf{R}') - H_{nn}(\mathbf{R}))^2} & (14) \\ &= \frac{2a^2}{\Delta^2} (1 - F(\mathbf{R}', \mathbf{R})) \cong (R'_i - R_i)(R'_j - R_j) \left\{ \frac{2N}{\pi^2} \frac{\partial^2 F}{\partial R'_i \partial R'_j} \Big|_{\mathbf{R}'=\mathbf{R}} \right\} \\ &= (\mathbf{R}' - \mathbf{R}) \cdot \mathbf{D}(\mathbf{R}) \cdot (\mathbf{R}' - \mathbf{R}). & (15) \end{aligned}$$

Eq. (15) demonstrates that on short distance scales, the evolution of the adiabatic energies of the Hamiltonian resemble a diffusion process, characterized by the *diffusion matrix*  $D_{ij}(\mathbf{R})$ . From the above definition,  $D_{ij}(\mathbf{R})$  can be related to the autocorrelation of the Hamiltonian or the local curvature properties of the energy surfaces:

$$D_{ij}(\mathbf{R}) = \overline{\nabla_i E_n(\mathbf{R}) \cdot \nabla_j E_n(\mathbf{R})} = \frac{2N}{\pi^2} \frac{\partial^2 F(\mathbf{R}', \mathbf{R})}{\partial R'_i \partial R'_j} \Big|_{\mathbf{R}'=\mathbf{R}}. \quad (16)$$

To obtain universality in correlation functions that depend on the parameters, we must rescale the parameters  $\mathbf{R}$ . In analogy to the 1-dimensional situation, we define:

$$\widetilde{\mathbf{R}} \equiv \mathbf{D}^{1/2} \cdot \mathbf{R} \quad (17)$$

Here  $\mathbf{D}^{1/2}$  is the *square root* of the diffusion matrix  $\mathbf{D}$  ( $\mathbf{D} = [\mathbf{D}^{1/2}]^T \mathbf{D}^{1/2}$ ), a model-dependent quantity. Because  $\overline{(\delta E_n)^2}$  is positive definite, it follows that the diffusion matrix  $D_{ij}(\mathbf{R})$  must be a positive definite matrix. As a consequence, its square root,  $\mathbf{D}^{1/2}$ , is always well defined. Specifically, it is an upper triangular matrix, which can be constructed using the Cholesky factorization[16]. In terms of  $\widetilde{\mathbf{R}}$ , the energy level diffusion is now parameter free:

$$\overline{(\delta E_n)^2} = \widetilde{\mathbf{R}}^2 \quad (18)$$

In analogy to the 1-dimensional scaling, we now expect all model dependence to be removed when we compute correlation functions in terms of  $\widetilde{\mathbf{R}}$ . These are in particular the dimension of the Hilbert space  $N$  and the short distance behavior of the autocorrelation function  $F(x) = 1 - cx^2 + \dots$  characterized by the coefficient(s)  $c$ . The rescaling by  $\mathbf{D}^{1/2}$  removes all this dependence, resulting in parameter free, *universal* results. We only remark here in passing that there is a more general class of processes for which the diffusion is not smooth[6], characterized by the short distance behavior of  $F(x)$ :  $F(x) = 1 - cx^\alpha + \dots$ , with  $0 \leq \alpha < 2$ . In this case, one can proceed as discussed above, but one must define the derivatives of  $F$  in Eq. (16) as fractional derivatives[17, 6].

In general, there is dependence of the diffusion matrix on its position in parameter space, clearly seen in Eq. (16). A general parametric Hamiltonian  $H(\mathbf{R})$  will have an autocorrelation  $F(\mathbf{R}', \mathbf{R})$  which is not translationally invariant, as is the case for the IBM Hamiltonian, so that  $D$  is parameter dependent. By construction, our random matrix Hamiltonian is translationally invariant, so that  $F(\mathbf{R}', \mathbf{R}) = F(\mathbf{R}' - \mathbf{R})$ , and as a result  $D_{ij}$  is independent of  $\mathbf{R}$ . We find for the random matrix model (Eq. 4):

$$D_{ij}(\mathbf{R}) = D_{ij} = D\delta_{ij} = \frac{N}{\pi^2}\delta_{ij} \quad (19)$$

In 1-parameter models,  $D_{ij} \rightarrow D_{xx} = C(0)$ , the scaling introduced in Refs. [3]. Note that our random matrix model is isotropic, which is certainly not the case for the IBM Hamiltonian, which contains bilinear parameter dependence of the form  $\eta\chi$ . In that case we compute the components of  $D_{ij}(\eta, \chi)$  for the energy surfaces  $E_n(\eta, \chi)$  and rescale accordingly.

Consider now the path taken from  $0 \rightarrow \widetilde{\mathbf{R}}$ . Each of the paths we follow between these points can develop a different geometric phase  $\gamma_n(\widetilde{\mathbf{R}})$ . Equivalently, we can consider closed circuits which begin and end at a given point, denoted  $\widetilde{\mathbf{R}} = 0$ . Using the two-parameter model in Eq. (4), where  $\mathbf{R} = (x, y)$ , we define such a path C as:

$$(0, 0) \rightarrow (X_0, 0) \rightarrow (X_0, Y_0) \rightarrow (0, Y_0) \rightarrow (0, 0) \quad (20)$$

Upon traversing this path, the wavefunction will develop a phase according to

$$|\psi_n\rangle \rightarrow e^{i\gamma_n(C)} |\psi_n\rangle = \pm |\psi_n\rangle. \quad (21)$$

From Eq. (19), the scaling along the circuit C in the  $x$  and  $y$  directions is:

$$\widetilde{R}_i = \sqrt{\frac{N}{\pi^2}}\delta_{ij}R_j, \quad \widetilde{x} = \sqrt{\frac{N}{\pi^2}}x, \quad \widetilde{y} = \sqrt{\frac{N}{\pi^2}}y. \quad (22)$$

The relevant quantity is the area of the loop,  $A = \Delta x \Delta y = X_0 Y_0$ . This quantity can be made more useful for comparisons to parametric areas in other Hamiltonians by defining the scaled area:

$$\widetilde{A} = \Delta \widetilde{x} \Delta \widetilde{y} = \sqrt{D_{xx} D_{yy}} X_0 Y_0. \quad (23)$$

As a check of our results, we plot in Fig. 1 the ratio of the computed value of  $\widetilde{A}$  to the predicted result in Eqs. (22),(23), using the Hamiltonian of Eq. (4), for varying sizes of the parametric loop. We take 100 points around the loop  $C$ , and compute  $D_{ij}(x, y)$  by

Figure 1: Comparison of computed scaled area,  $\tilde{A} = \sqrt{D_{xx}D_{yy}}X_0Y_0$ , of the parametric loop  $C$ , for the Hamiltonian of Eq. (4), to the theoretical result from Eqs. (22)-(23). The dashed line is the expected result.

averaging over the middle third of the energy surfaces  $E_n(x, y)$ . The agreement is quite good. (There is a slight systematic shift of the results which seems to be due to the method used to unfold the energy spectrum.)

The regime of universality is roughly defined by the scale [4]

$$|\widetilde{\mathbf{R}}| \lesssim 1. \quad (24)$$

Analogously, the regime of universal behavior for topological phase accumulation is

$$\tilde{A} \lesssim 1. \quad (25)$$

We will see in the next section, that the area of the loop does not have to be large before one finds significant effects, and saturation of these effects already occur within the universal regime.

Our previous work in Refs. [7, 4] examined the universal statistical decorrelations of wavefunction related observables in a one parameter formalism. In Fig. 2, a typical universal result is shown for the distribution of wavefunction overlaps,  $P(u; \widetilde{\mathbf{R}})$ , with  $u = \langle \psi_n(\widetilde{\mathbf{R}}) | \psi_n(0) \rangle$ , for a 1-parameter path. (The vertical axis in all plots of  $P(u; \widetilde{\mathbf{R}})$  is rescaled to place the maximum near unity.) The solid histogram is the result from random matrix theory, and the dashed histogram is the result from the IBM, in particular  $J^\pi = 10^+$  states [7]. Using  $N_b = 25$ , this corresponds to a dimension of 211 states, of which only the middle third of the eigenstates are used. The distribution begins as a delta function at  $\widetilde{\mathbf{R}} = 0$ , and develops into a Porter-Thomas distribution for  $\widetilde{\mathbf{R}} \gg 1$ . The Porter-Thomas limit is non-universal in the sense that the distribution depends explicitly on the dimension  $N$  of the space. A one-dimensional path in the 2-dimensional parameter space (Eq. 9) has the same universal behavior when plotted as a function of the scaled distance  $\widetilde{\mathbf{R}} = \mathbf{D}^{\frac{1}{2}} \cdot \mathbf{R}$ . However, if we now allow paths in two or more dimensions, the shape of this distribution depends on *how* one reaches the position  $\widetilde{\mathbf{R}}$ .

Consider the same distributions when we traverse the path of Eq. (20) of area  $\tilde{A}$ . When we transport  $N$  eigenstates around the loop, a certain number of them will develop a phase  $\gamma_n(C) = \pi$ , which we denote  $\mathcal{N}(\pi)$ . The remaining  $\mathcal{N}(0)$  states do not acquire a phase, where  $N = \mathcal{N}(0) + \mathcal{N}(\pi)$ . The fraction of states which acquire a Berry's phase is defined as:

$$f = \frac{\mathcal{N}(\pi)}{\mathcal{N}(0) + \mathcal{N}(\pi)}. \quad (26)$$

As mentioned above, because a non-zero value for  $\mathcal{N}(\pi)$  indicates that paths followed by certain eigenstates enclose a diabolical point, this measure is clearly related to the number of diabolical points enclosed by the path of area  $A$ . In Fig. 3, the wavefunction overlap distribution function,  $P(u; \widetilde{\mathbf{R}})$ , is shown at various points along the square circuit  $C$ . The solid histogram corresponds to the random matrix predictions, and the dots to the results from the IBM. Initially, the distribution is a delta function centered at  $(x, y) = (0, 0)$ . As the separation increases, the decorrelation is similar to the results of Fig. 2. But as the circuit returns to the origin, the distribution bifurcates into two distinct distributions, corresponding to the existence of the Berry's phase of  $\pm 1$ . As the circuit is closed, the distribution does not go back to its original form, but is now described by two delta functions located at  $\pm 1$  of equal magnitudes (within numerical fluctuations). The



Figure 2: One-parameter universality of the distribution of matrix elements  $P(u; \widetilde{\mathbf{R}})$ , where  $u = \langle \psi_n(\widetilde{\mathbf{R}}) | \psi_n(0) \rangle$ . The solid histogram is random matrix prediction while the dotted histogram is the observed result from the Interacting Boson Model[7].

fraction  $f$  is at its saturation value of 50% for this loop, as seen in Fig. 3(f). Hence, the short distance universality that occurs in multiparameter systems is not simply a function of the metric distance between the two points 0 and  $\widetilde{\mathbf{R}}$ . Given only the distance  $\widetilde{\mathbf{R}}$ , the distribution  $P(u; \widetilde{\mathbf{R}})$  is not well defined, since one might be close to either Fig. 3(a) or 3(f), which represent the same point. However, both are universal results when one follows a path of the same scaled area. In this case, the universal function  $P(u)$  must also identify the area subtended by the path. Figure 4 shows a similar collection of distributions in the case of a smaller parametric square. As can be seen here, only a small fraction of states subtend a diabolical point. It is clear that quantities which are sensitive to the phase of the wavefunctions will generally be modified in multi-parameter theories.

#### 4. Universal Density of Diabolical Points

The effect we have described in the previous section is due to diabolical points which are enclosed by the parametric paths. We now consider the density of these diabolical points. It has been shown that a necessary condition for the occurrence of a Berry's phase of  $\gamma(C) = \pi$  for a system transported around a closed loop  $C$  is the existence of a diabolical point within the loop[9, 10]. Hence the fraction  $f$  of states in Fig. 3(f) and 4(d) that have  $\gamma(C) = \pi$  should be a measure of the number of diabolical points enclosed in the area  $A$ , or equivalently, the density of diabolical points. We note that we assume that as the area increases, the occurrence of a new diabolical point is responsible for the phase change of only one eigenfunction. For loops of small area, which is the situation in the universal regime, this is a reasonable assumption. In Fig. 5 (top) we plot the fraction of states  $f$  which enclose a diabolical point as a function of the scaled area. There are three sets of results in the figure. The crosses are the result of varying the size of the loop,  $X_0 = Y_0 \in (0, 0.25]$ , with  $N = 200$ , so that the scaled area varies from 0 to 1.27. The boxes correspond to varying the dimension of the matrices from  $N = 50 - 300$ , for fixed area with  $X_0 = Y_0 = 0.18$ . Finally, the open circles correspond to parametric loops in the Interacting Boson Model, at fixed dimension. As is clearly seen the behavior is statistically equivalent for all the results, demonstrating universality of the results. The general features of these results are the following. We see that the fraction  $f$  increases linearly with scaled area, and that statistical saturation of 50% occurs for  $\widetilde{A} \sim 1$ . (In the Hamiltonian (4), the relation to the area is  $\widetilde{A} = NA/\pi^2$  (see Fig. 1) while in the IBM,  $\widetilde{A} \propto NA$ .) We expect saturation when there are many diabolical points, so that statistically the probability of having a phase change for an arbitrary wavefunction is  $1/2$ . If we define the number of diabolical points enclosed by the circuit  $C$  as  $n(C) = Nf(C)$ , we conclude that in the non-saturation regime,

$$f(C) = cNA, \quad n(C) = cN^2A, \quad (27)$$

where  $c$  is determined from the slope of Fig. 5 (bottom). In the saturation regime,

$$f(C) = \frac{1}{2}, \quad n(C) = \frac{N}{2}. \quad (28)$$

Figure 3: Modification of 1-parameter universality for a 2 parameter square of side  $X_0 = Y_0 = 0.32$ , with  $N=200$ . The distribution  $P(u; \tilde{\mathbf{R}})$  is shown at the points  $(X,Y) =$  (a)  $(0,0)$ , (b)  $(0.16,0)$ , (c)  $(0.32,0.32)$ , (d)  $(0,0.32)$ , (e)  $(0,0.16)$ , (f)  $(0,0)$  (after traversal of loop). Both (f) and (a) represent the same point, showing that universality is path dependent. The dotted histogram corresponds to results from the IBM, on a parametric loop of similar scaled area.

Figure 4: Same as Fig. 3, but for a loop of smaller area. In this case,  $X_0 = Y_0 = 0.03$ , and  $N = 200$ . The figures correspond to  $(X, Y) =$  ( in units of  $X_0$ ) (a)  $(0, 0)$ , (b)  $(1.0, 1.0)$ , (c)  $(0.8, 1.0)$ , (d)  $(0, 0)$  (after traversal of loop). The smaller loop area contains fewer diabolical points and hence has fewer states which split in (d). The dashed histogram corresponds to the results from the IBM, which are plotted slightly offset for better contrast.

When the area is large,  $f$  is no longer a good measure of the number of diabolical points, so the dependence of  $n(C)$  and  $f(C)$  with  $N$  is no longer meaningful. In Fig. 5 (bottom), we plot the small area behavior of the fraction  $f$ . The statistical errors are computed by computing the fraction  $f$  and the scaled area  $\tilde{A}$  for a number of realizations of the parametric Hamiltonians. The results for the chaotic system (IBM), the open circles, are not averaged over, but come from a single parametric loops. The general result is that the number of diabolical points grows quadratically with the dimension of the matrix. (Saturation effects occur for larger areas). From the results of Fig. 5, we conclude that the fractional density of diabolical points,  $\rho$ , in terms of scaled area, is a universal constant for chaotic systems, given by

$$\rho \equiv \frac{f(C)}{\tilde{A}} = 0.94 \pm 0.10 \quad (29)$$

The quantity similar to  $n(C)$  was examined recently in a very interesting study of avoided level crossings [10], using the same two-parameter GOE model. In that study, a similar scaling in  $N$  was found for the number of diabolical points, although their results were not universal, and do not completely agree with the results of this study. The overall scaling agreement is encouraging, and we believe the discrepancy is due to the different methods used to count diabolical points.

## 5. Conclusions

We have developed a formalism to compute universal parametric correlations in multi-parameter systems, explicitly demonstrating universality in chaotic systems. The scaling is achieved through the square root of the diffusion matrix  $D_{ij}$ . We have also found that universal results for two-point correlation functions and distributions, which are thought to be only a function of the separation of the points in parameter space, can be path dependent in more than one parameter dimension. Indeed, one can obtain distinct results for the universal correlations by reaching the same final point by different paths. So short distance correlations are not a simple function of the metric distance between the points in parameter space, but are also a function of the shape of the path taken between the points. This is true for all quantities which are sensitive to the phase of the wavefunctions. Whether one can actually measure interference effects in a manner analogous to measures of Berry's phase is an interesting question to explore. Quantities which are not sensitive to the phase, will not suffer from this ambiguity. Finally, we have verified that the density of diabolical points grows quadratically with the dimension of the matrix, and used that to determine a universal measure of the density of diabolical points in chaotic systems.

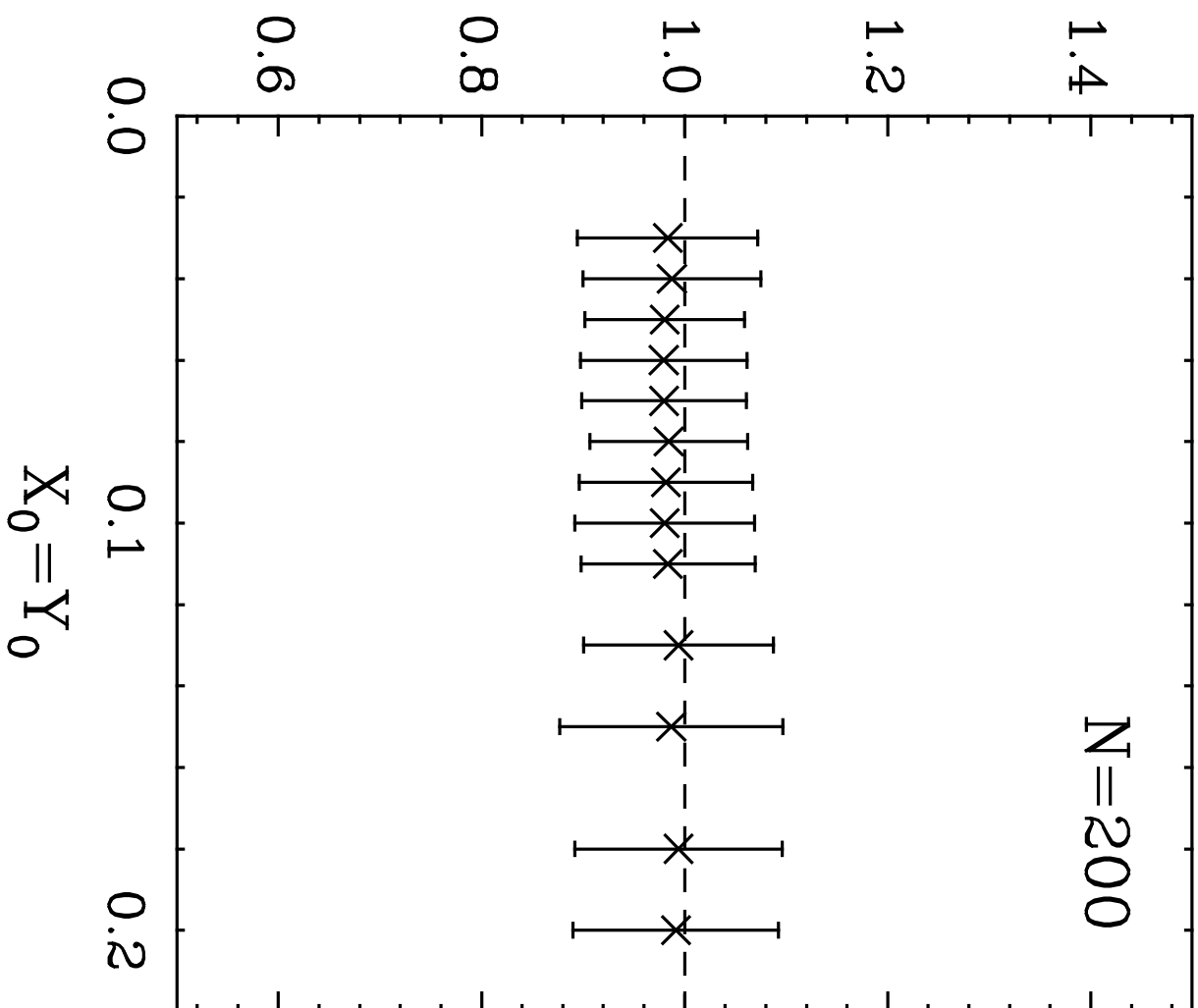
This work was supported in part by the Department of Energy Grant DE-FG02-91ER40608.

Figure 5: Universality of the fractional number of diabolical points  $f$ . (top) Fraction of wavefunctions enclosing a diabolical point as a function of the scaled area of the loop  $C$ , calculated at (i) fixed dimension  $N = 200$ , with the size of the loop varying over the range  $0 \leq X_0 = Y_0 \leq 0.25$  (crosses); (ii) fixed loop area with  $X_0 = Y_0 = 0.18$ , and the dimension varied from  $N = 25 - 300$  (boxes); (iii) fixed dimension in the chaotic region of the IBM parameter space, for several loop sizes (circles). (bottom) Linear behavior of the small area behavior of  $f$ . From this we find the the density of diabolical points increases quadratically with the dimension of the matrix.

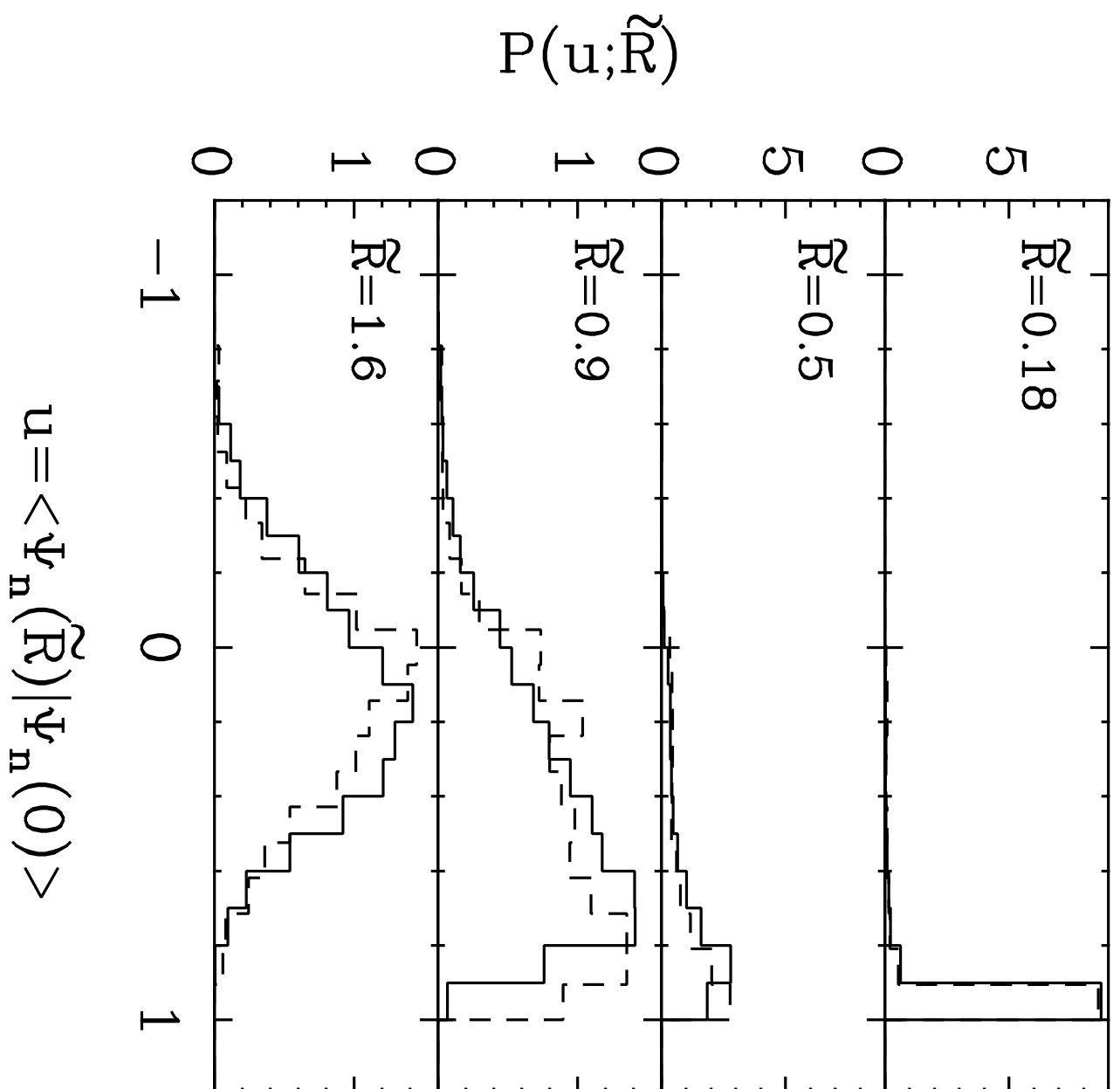
## References

- [1] See for example, O. Bohigas, in *Chaos and Quantum Physics*, Eds. M. Giannoni, A. Voros and J. Zinn-Justin, (North-Holland, New York, 1991).
- [2] H. Weidenmüller, in *Progress in Particle and Nuclear Physics*, V.**3**, 49 (Pergamon, Oxford, 1980); A. Bulgac, G.DoDang and D.Kusnezov, *Ann. Phys. (NY)* **A242** (1995) 1.
- [3] A. Szafer and B. L. Altshuler, *Phys. Rev. Lett.* **70**, 587 (1993); B.D. Simons and B.L. Altshuler, *Phys. Rev. Lett.* **70**, 4063 (1993); *Phys. Rev. B* **48**, 5422 (1993). B.D. Simons, P.A. Lee and B.L. Altshuler, *Phys. Rev. Lett.* **70** 4122 (1993); *ibid* **72**, 64 (1994); *Nucl. Phys.* **B409**, 487 (1993).
- [4] D.Mitchell, Y.Alhassid, and D.Kusnezov, *Phys. Lett. A* (in press) (1996).
- [5] Y.Alhassid and H.Attias, *Phys. Rev. Lett.* **74** (1995) 4635.
- [6] D.Kusnezov and C.Lewenkopf, *Phys. Rev.* **E53** (1996) 2283.
- [7] D. Kusnezov and D.Mitchell, nucl-th/9510002 (1995).
- [8] M.V. Berry, *Proc, Roy. Soc. Lond.* **A392** (1984) 45; A. Shapere and F. Wilczek, *Geometric Phases in Physics*, (World Scientific, New Jersey, 1989).
- [9] M.V. Berry and M. Wilkinson, *Proc, Roy. Soc. Lond.* **A392** 15 (1984)
- [10] E. Austin and M. Wilkinson, *Nonlinearity* **5** (1992) 1137 ; M. Wilkinson and E. Austin, *Phys. Rev.* **A47** (1993) 2601.
- [11] F. Iachello and A. Arima, *The Interacting Boson Model* (Cambridge Press, Cambridge, 1987).
- [12] R. Casten and D.D.Warner, *Rev. Mod. Phys.* **60** (1988) 389; P.O.Lipas, P. Toivonen and D.D.Warner, *Phys. Lett.* **B155** (1985) 295; Y.Alhassid and N.Whelan, *Phys. Rev. Lett.* **67** (1991) 816.
- [13] Y.Alhassid, N.Whelan and A.Novoselsky, *Mod. Phys. Lett.* **A7**, 2453 (1992).
- [14] J.P.Provost and G.Vallee, *Comm. Math. Phys.* **76** (1980) 289.
- [15] F.J. Dyson, *J. Math. Phys.* **3**, 1191 (1962).
- [16] D. Jacobs, *The State of the Art in Numerical Analysis*, (Academic Press, London, 1979).
- [17] B. Ross, *Fractional Calculus and its Applications*, (Springer-Verlag, New York, 1974); K. S. Miller and B. Ross, *An introduction to the fractional calculus and fractional differential equations*, (Wiley, New York, 1993).

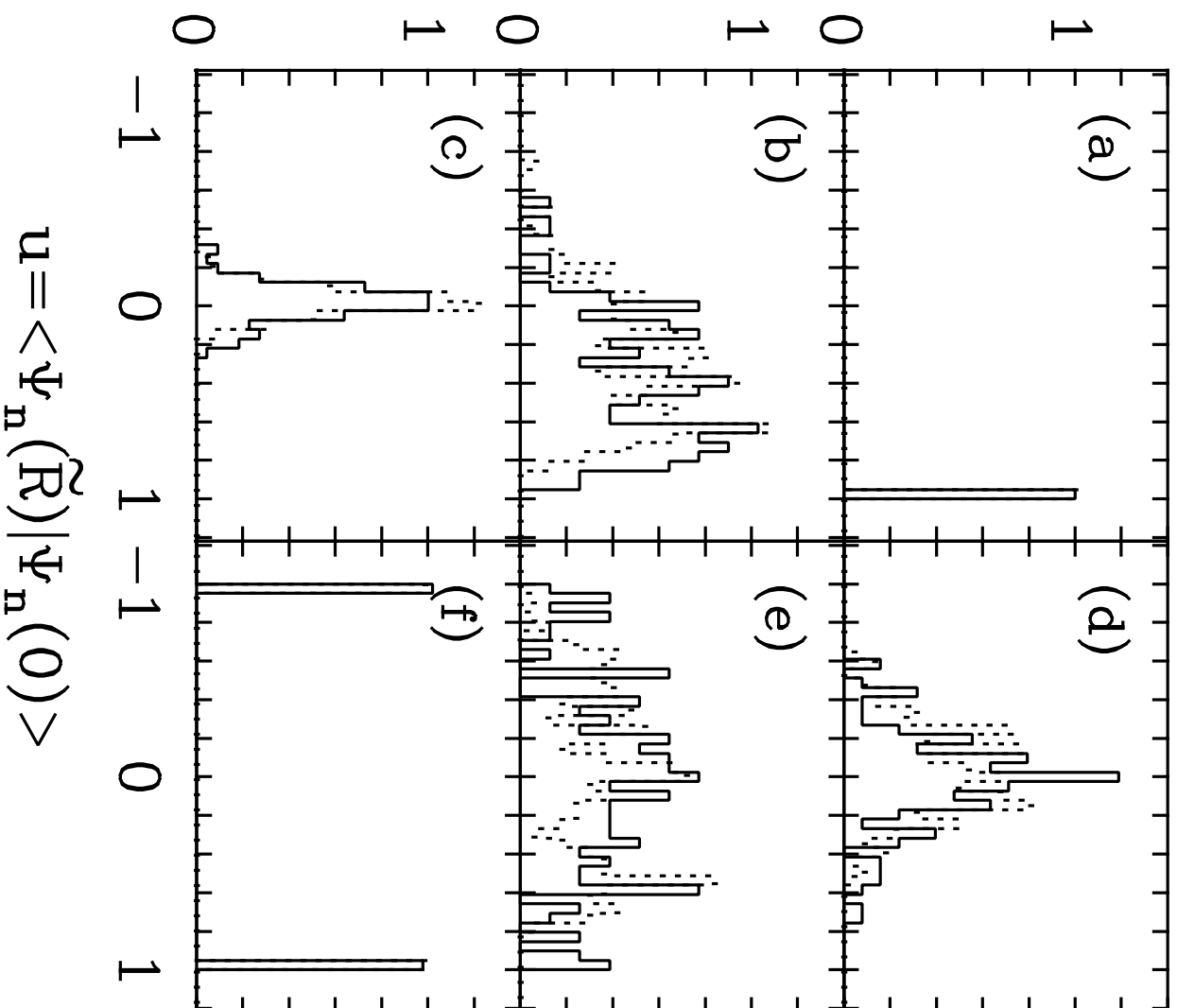
$$[D_{xx}D_{yy}]^{1/2}\pi^2/N$$



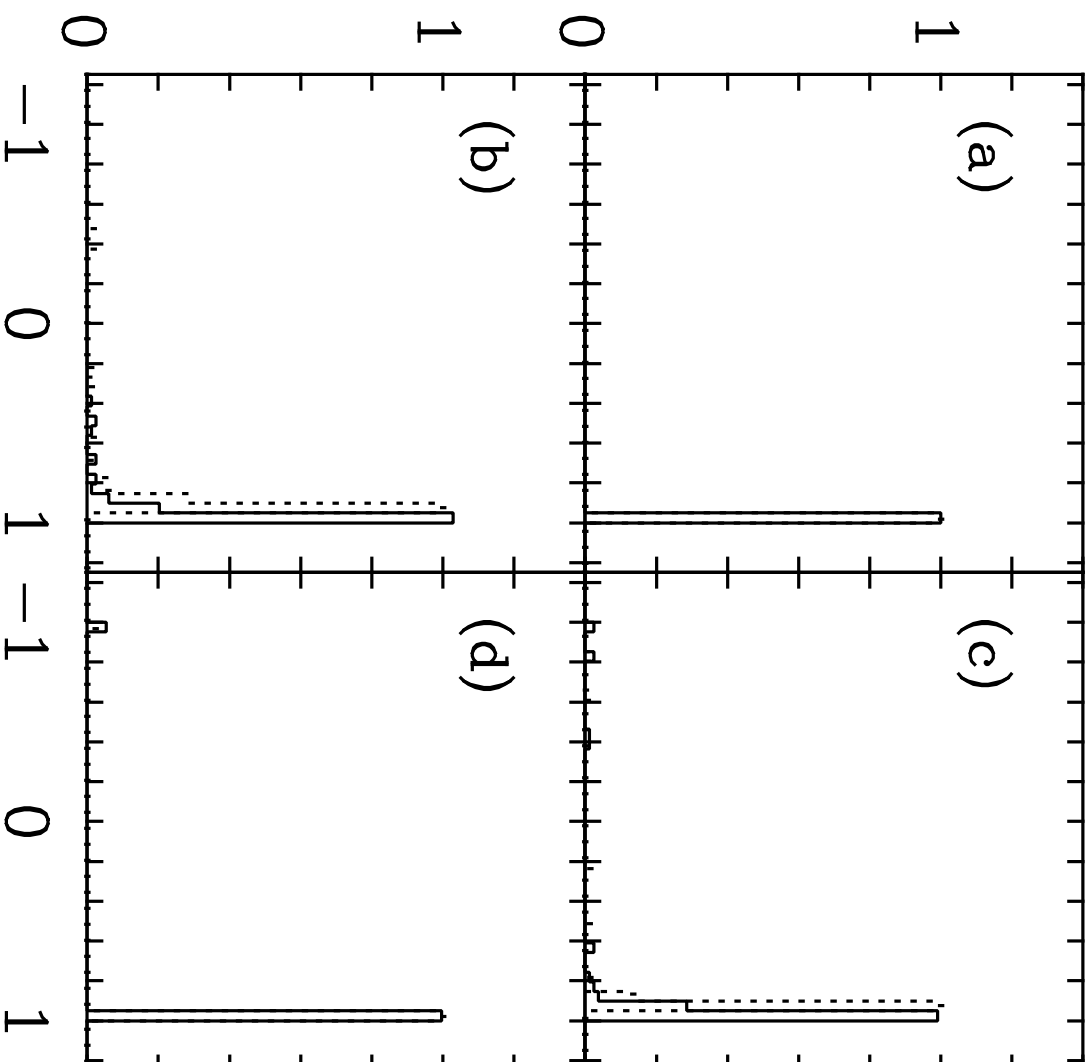




$P(u; \tilde{R})$



$P(u; \tilde{R})$



$u = \langle \Psi_n(\tilde{R}) | \Psi_n(0) \rangle$

$n(C)/N$  (%)

